Phonon modes and melting properties of two-dimensional Penrose lattices

Xiuqing Huang*
Department of Physics, South China University of Technology, 510641, People's Republic of China

Youyan Liu
Chinese Center of Advanced Science and Technology (World Laboratory), P.O. Box 8730, Beijing 100080, People's Republic of China and Department of Physics, South China University of Technology, Guangzhou, 510641, People's Republic of China†

Nanzhi Zou
Department of Physics, Tronheim University, Tronheim, Norway

Penghui Ma
Department of Physics, Trent University, Peterborough, Canada
(Received 22 July 1991; revised manuscript received 25 June 1992)

We study the phonon modes and melting properties of two-dimensional Penrose lattices with fivefold rotational symmetry. We use a similarity transformation to reduce the numerical calculations, which also helps us determine analytically the degeneracies of the phonon modes. It is found that two-thirds of the modes are doubly degenerate and the remaining one-third nondegenerate. Using the mean-square atomic-displacement criterion of Lindemann, we have studied the melting properties of two-dimensional Penrose lattices and found that the boundary atoms always have a lower melting temperature than those in the bulk.

I. INTRODUCTION

The discovery of a quasicrystalline phase in Al-Mn alloys by Schechtman *et al.*[1] in 1984, which give a diffraction pattern with peaks showing icosahedral symmetry, has led to widespread interest in quasicrystalline systems.[2–10] Many results on the electronic and phonon properties of two-dimensional quasicrystalline systems have been reported in recent years:[11–17] The lattice vibrational properties of two-dimensional quasicrystalline systems have been numerically studied by various authors. Odagaki and Nguyen[14] have studied the lattice vibrations of Penrose lattices constructed with kites and darts perpendicular to the lattice plane and found energy gaps in the spectrum due to the aperiodic structure. Kohmoto and Sutherland[15] have investigated the existence of localized modes in a system similar to that of Odagaki *et al.* Nishiguchi and Sakuma[16] studied the vibrational spectra and energy distribution of Penrose lattices with fivefold rotational symmetry constructed with fat and thin rhombi, but they have not investigated the degeneracy of the phonon spectrum resulting from the fivefold rotational symmetry of these systems. On the other hand, no theoretical study has been reported on the melting properties of the quasicrystalline systems, especially from the view point of lattice dynamics. It is well known that for a two-dimensional *infinite* periodic system, the mean-square atomic displacement (MSD) diverges logarithmically as the number of atoms increases. Because the structural stability of a Penrose quasiperiodic system is lower than that of a regular system, a higher degree of divergence is expected. Therefore a three-dimensional model should be far more reliable to use in dealing with melting problems. However, because of the complicated geometric structure of quasiperiodic lattices, one cannot in general obtain analytic solutions for the problems under study even for their one-dimensional counterparts. On the other hand, the capacity of present-day computers (even supercomputers) cannot handle a three-dimensional quasiperiodic system of a reasonable size; therefore as a first step in the theoretical study of these systems, we consider the melting properties of a two-dimensional Penrose system of finite size, by using the Lindemann criterion. Penrose quasilattices with fivefold rotational symmetry can be obtained by the generalized dual method (GDM) from a periodic pentagrid[18] (see Fig. 1). For the study of phonon modes of Penrose lattices, there are primarily two kinds of model: the center model and the vertex model.[11,12] In the present paper, we concentrate on the vertex model, whose atoms are located at vertices of the rhombi. In Sec. II we first present the dynamical matrices of these systems, then introduce a similarity transformation to put the dynamical matrices in block-diagonal form, which helps us draw some conclusions analytically on the degeneracy of the phonon spectrum and which leads to remarkable savings in computing time and a reduction in the computer memory required. In Sec. III we use the block-diagonal method to calculate the density of states of these two-dimensional Penrose lattices. In Sec. IV we use the mean-square atomic displacement (MSD) criterion of Lindemann to study the melting properties of the two-dimensional Penrose lattices that have been extensively used to model the melting transition of surfaces and the bulk.[19–22]

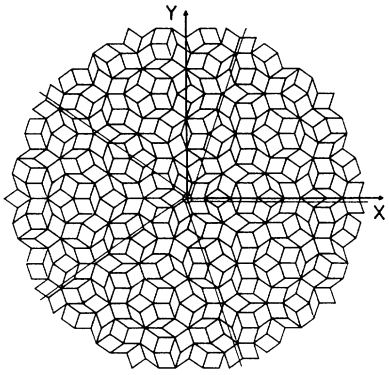

FIG. 1. The Penrose lattice with fivefold rotational symmetry studied. The number of vertices (atoms) is $N=471$.

II. REDUCTION OF DYNAMICAL MATRIX AND DEGENERACIES OF SPECTRUM

For two-dimensional Penrose lattices with fivefold rotational symmetry, we can divide the lattice into five identical wedge sublattices, all of which share the central atom (Fig. 1).[11] Assume that in every sublattice there are N_1 atoms, and an interaction exists only between adjacent sublattices. We label the atoms of the five identical wedge sublattices in the same way; then the dynamical matrix $\underline{D}$ can be written as follows in Eq. (2.1). Here

$$\underline{C}_0=\begin{bmatrix} a & 0 \\ 0 & a \end{bmatrix}$$

is a 2×2 matrix corresponding to the central atom. $\underline{t}_1,\underline{t}_2,\ldots,\underline{t}_{N_1}$, which are the interaction matrices between the central atom and atoms of the first wedge sublattices, are also 2×2 matrices. $\underline{A}_0$ is a $2N_1\times2N_1$ dynamical matrix for the first wedge sublattices. $\underline{H}$ is the interaction matrix between the first and second wedge sublattices, which is also a $2N_1\times2N_1$ matrix. $\underline{H}^T$ is the transpose of matrix $\underline{H}$. In formula (2.1), the 2×2 matrices $\underline{u}_k$ and $2N_1\times2N_1$ block-diagonal matrices $\underline{V}_k$ are, respectively,

$$\underline{u}_k=\begin{bmatrix} \cos(2k\pi/5) & \sin(2k\pi/5) \\ \sin(2k\pi/5) & \cos(2k\pi/5) \end{bmatrix}, \tag{2.2a}$$

$$\underline{V}_k=\underline{1}_{N_1\times N_1}\otimes\underline{u}_k, \text{ with } k=1,2,3, \text{ and } 4, \tag{2.2b}$$

where $\underline{1}_{N_1\times N_1}$ is the $N_1\times N_1$ unit matrix. Now we introduce a transformation matrix $\underline{P}$ as the following:

$$\underline{P}=\frac{1}{\sqrt{5}}\begin{bmatrix} \sqrt{\frac{5}{2}}\begin{bmatrix} i & -1 \\ i & 1 \end{bmatrix} & \underline{0}_{2\times2N_1} & \underline{0}_{2\times2N_1} & \underline{0}_{2\times2N_1} & \underline{0}_{2\times2N_1} & \underline{0}_{2\times2N_1} \\ \underline{0}_{2N_1\times2} & \underline{1}_{2N_1\times2N_1} & \underline{V}_1 & \underline{V}_2 & \underline{V}_3 & \underline{V}_4 \\ \underline{0}_{2N_1\times2} & \underline{1}_{2N_1\times2N_1} & \varepsilon_1\underline{V}_1 & \varepsilon_2\underline{V}_2 & \varepsilon_3\underline{V}_3 & \varepsilon_4\underline{V}_4 \\ \underline{0}_{2N_1\times2} & \underline{1}_{2N_1\times2N_1} & \varepsilon_1^2\underline{V}_1 & \varepsilon_2^2\underline{V}_2 & \varepsilon_3^2\underline{V}_3 & \varepsilon_4^2\underline{V}_4 \\ \underline{0}_{2N_1\times2} & \underline{1}_{2N_1\times2N_1} & \varepsilon_1^3\underline{V}_1 & \varepsilon_2^3\underline{V}_2 & \varepsilon_3^3\underline{V}_3 & \varepsilon_4^3\underline{V}_4 \\ \underline{0}_{2N_1\times2} & \underline{1}_{2N_1\times2N_1} & \varepsilon_1^4\underline{V}_1 & \varepsilon_2^4\underline{V}_2 & \varepsilon_3^4\underline{V}_3 & \varepsilon_4^4\underline{V}_4 \end{bmatrix}, \tag{2.3}$$

where $\underline{1}_{2N_1\times2N_1}$ is the $2N_1\times2N_1$ unit matrix, $\underline{V}_k$, with $k=1,2,3$, and 4, are $2N_1\times2N_1$ matrices, and $\varepsilon_k=\exp(i2\pi k/5)$, with $k=1,2,3$, and 4, are the fifth roots of unity.

Then matrix $\underline{P}\,\underline{D}\,\underline{P}^{-1}$ is given as

$$\underline{P}\,\underline{D}\,\underline{P}^{-1}=\begin{bmatrix} a & 0 & \underline{0}_{1\times2N_1} & \underline{0}_{1\times2N_1} & \underline{0}_{1\times2N_1} & \underline{0}_{1\times2N_1} & \frac{\sqrt{10}}{2}\begin{bmatrix} i \\ -1 \end{bmatrix}^T\underline{T} \\ 0 & a & \underline{0}_{1\times2N_1} & \frac{\sqrt{10}}{2}\begin{bmatrix} i \\ 1 \end{bmatrix}^T\underline{T} & \underline{0}_{1\times2N_1} & \underline{0}_{1\times2N_1} & \underline{0}_{1\times2N_1} \\ \underline{0}_{2N_1\times1} & \underline{0}_{2N_1\times1} & \underline{A}_1' & \underline{0} & \underline{0} & \underline{0} & \underline{0} \\ \underline{0}_{2N_1\times1} & \frac{\sqrt{10}}{2}\underline{T}^T\begin{bmatrix} -i \\ -1 \end{bmatrix} & \underline{0} & \underline{A}_2' & \underline{0} & \underline{0} & \underline{0} \\ \underline{0}_{2N_1\times1} & \underline{0}_{2N_1\times1} & \underline{0} & \underline{0} & \underline{A}_3' & \underline{0} & \underline{0} \\ \underline{0}_{2N_1\times1} & \underline{0}_{2N_1\times1} & \underline{0} & \underline{0} & 0 & \underline{A}_4' & \underline{0} \\ \frac{\sqrt{10}}{2}\underline{T}^T\begin{bmatrix} -i \\ -1 \end{bmatrix} & \underline{0}_{2N_1\times1} & \underline{0} & \underline{0} & \underline{0} & \underline{0} & \underline{A}_5' \end{bmatrix}, \tag{2.4}$$

$$
\underline{D}=\left\{\begin{array}{c|cccc}
\underline{C}_0 & \underline{t}_1 \cdots \underline{t}_{N_1} & \underline{u}_1^T\underline{t}_1\underline{u}_1 \cdots \underline{u}_1^T\underline{t}_{N_1}\underline{u}_1 & \underline{u}_2^T\underline{t}_1\underline{u}_2 \cdots \underline{u}_2^T\underline{t}_{N_1}\underline{u}_2 & \underline{u}_3^T\underline{t}_1\underline{u}_3 \cdots \underline{u}_3^T\underline{t}_{N_1}\underline{u}_3 & \underline{u}_4^T\underline{t}_1\underline{u}_4 \cdots \underline{u}_4^T\underline{t}_{N_1}\underline{u}_4 \\
\underline{t}_1^T & & & & & \\
\vdots & \underline{A}_0 & \underline{H} & \underline{0}_{2N_1\times 2N_1} & \underline{0}_{2N_1\times 2N_1} & \underline{V}_4^T\underline{H}^T\underline{V}_4 \\
\underline{t}_{N_1}^T & & & & & \\
\underline{u}_1^T\underline{t}_1^T\underline{u}_2 & & & & & \\
\vdots & \underline{H}^T & \underline{V}_1^T\underline{A}_0\underline{V}_1 & \underline{V}_1^T\underline{H}\underline{V}_1 & \underline{0}_{2N_1\times 2N_1} & \underline{0}_{2N_1\times 2N_1} \\
\underline{u}_1^T\underline{t}_{N_1}^T\underline{u}_1 & & & & & \\
\underline{u}_2^T\underline{t}_1^T\underline{u}_2 & & & & & \\
\vdots & \underline{0}_{2N_1\times 2N_1} & \underline{V}_1^T\underline{H}^T\underline{V}_1 & \underline{V}_2^T\underline{A}_0\underline{V}_2 & \underline{V}_2^T\underline{H}\underline{V}_2 & \underline{0}_{2N_1\times 2N_1} \\
\underline{u}_2^T\underline{t}_{N_1}^T\underline{u}_2 & & & & & \\
\underline{u}_3^T\underline{t}_1^T\underline{u}_3 & & & & & \\
\vdots & \underline{0}_{2N_1\times 2N_1} & \underline{0}_{2N_1\times 2N_1} & \underline{V}_2^T\underline{H}^T\underline{V}_2 & \underline{V}_3^T\underline{A}_0\underline{V}_3 & \underline{V}_3^T\underline{H}\underline{V}_3 \\
\underline{u}_3^T\underline{t}_{N_1}^T\underline{u}_3 & & & & & \\
\underline{u}_4^T\underline{t}_1^T\underline{u}_4 & & & & & \\
\vdots & \underline{V}_4^T\underline{H}\underline{V}_4 & \underline{0}_{2N_1\times 2N_1} & \underline{0}_{2N_1\times 2N_1} & \underline{V}_3^T\underline{H}^T\underline{V}_3 & \underline{V}_4^T\underline{A}_0\underline{V}_4 \\
\underline{u}_4^T\underline{t}_{N_1}^T\underline{u}_4 & & & & &
\end{array}\right\} \tag{2.1}
$$

where $\underline{T}=(\underline{t}_1 \cdots \underline{t}_{N_1})$, which is the interaction matrix between the central atom and atoms of the first wedge sublattices, is a $2\times N_1$ matrix. The $2N_1\times 2N_1$ submatrices $\underline{A}_i'$, with $i=1,2,3,4$, and 5, are, respectively,

$$\underline{A}_1'=\underline{A}_0+\underline{V}_1\underline{H}^T+\underline{H}\,\underline{V}_1^T , \tag{2.5a}$$

$$\underline{A}_2'=\underline{A}_0+\varepsilon_4\underline{V}_1\underline{H}^T+\varepsilon_4\underline{H}\,\underline{V}_1^T , \tag{2.5b}$$

$$\underline{A}_3'=\underline{A}_0+\varepsilon_2\underline{V}_1\underline{H}^T+\varepsilon_2^*\underline{H}\,\underline{V}_1^T , \tag{2.5c}$$

$$\underline{A}_4'=\underline{A}_0+\varepsilon_3\underline{V}_1\underline{H}^T+\varepsilon_3^*\underline{H}\,\underline{V}_1^T , \tag{2.5d}$$

$$\underline{A}_5'=\underline{A}_0+\varepsilon_4\underline{V}_1\underline{H}^T+\varepsilon_4^*\underline{H}_1\underline{V}^T , \tag{2.5e}$$

and we obtain the submatrices $\underline{A}_i$, with $i=1,2,3,4$, and 5, as follows:

$$\underline{A}_1=\underline{A}_1' . \tag{2.6a}$$

$$\underline{A}_2=\begin{bmatrix} a & \frac{\sqrt{10}}{2}\begin{bmatrix} i \\ 1 \end{bmatrix}^T\underline{T} \\ \frac{\sqrt{10}}{2}\underline{T}^T\begin{bmatrix} -i \\ -1 \end{bmatrix} & \underline{A}_2' \end{bmatrix} , \tag{2.6b}$$

$$\underline{A}_3=\underline{A}_3' , \tag{2.6c}$$

$$\underline{A}_4=\underline{A}_4' , \tag{2.6d}$$

$$\underline{A}_5=\begin{bmatrix} a & \frac{\sqrt{10}}{2}\begin{bmatrix} i \\ -1 \end{bmatrix}^T\underline{T} \\ \frac{\sqrt{10}}{2}\underline{T}^T\begin{bmatrix} -i \\ -1 \end{bmatrix} & \underline{A}_5' \end{bmatrix} . \tag{2.6e}$$

Evidently, the eigenvalues of the dynamical matrix $\underline{D}$ are the sum of those of $\underline{A}_1$, $\underline{A}_2$, $\underline{A}_3$, $\underline{A}_4$, and $\underline{A}_5$. Because

$$\varepsilon_2=\varepsilon_5^* \quad \text{and} \quad \varepsilon_3=\varepsilon_4^* ,$$

we have

$$\underline{A}_2=\underline{A}_5^* \quad \text{and} \quad \underline{A}_3=\underline{A}_4^* .$$

On the other hand, $\underline{A}_i$'s are Hermitian; consequently, $\underline{A}_2$ and $\underline{A}_5$, and $\underline{A}_3$ and $\underline{A}_4$, have identical eigenvalue spectrum, but $\underline{A}_1$ has an independent spectrum. We can conclude that for two-dimensional Penrose lattices with fivefold rotational symmetry, two-thirds of the states of the phonon spectra are doubly degenerate and one-third of the modes are nondegenerate. This result is in agreement with that of the numerical simulation.

If $\mathbf{X}_1$, $\mathbf{X}_2$, and $\mathbf{X}_3$ are used to denote, respectively, the eigenvectors of the first, second, and third submatrix, then the corresponding eigenvectors $\mathbf{X}(j)$ for the whole system can be constructed by the sub-eigenvector $\mathbf{X}_i$. For different $\mathbf{X}_i$, the $\mathbf{X}(j)$ has a different expression shown as follows:

$$\mathbf{X}(j)=(1/\sqrt{5})\bigoplus_{k=0}^{4}\underline{V}_k\mathbf{X}_1 , \tag{2.7}$$

$$\mathbf{X}(j)=\mathrm{Re}(\sqrt{\tfrac{2}{5}}\bigoplus_{k=0}^{4}\underline{V}_k\varepsilon_k\mathbf{X}_3) , \tag{2.8a}$$

$$\mathbf{X}(j)=\mathrm{Im}(\sqrt{\tfrac{2}{5}}\bigoplus_{k=0}^{4}\underline{V}_k\varepsilon_k\mathbf{X}_2) , \tag{2.8b}$$

$$\mathbf{X}(j)=\mathrm{Re}\left[\frac{1}{\sqrt{2}}\begin{bmatrix} i & i \\ 1 & -1 \end{bmatrix}\begin{bmatrix} x(1) \\ x(2) \end{bmatrix}\right] \oplus \mathrm{Re}\left[\sqrt{\tfrac{2}{5}}\bigoplus_{k=0}^{4}\underline{V}_k\,\varepsilon_k^4\mathbf{x}_2\right] , \tag{2.9a}$$

$$\mathbf{X}(j)=\mathrm{Im}\left[\frac{1}{\sqrt{2}}\begin{bmatrix} i & i \\ 1 & -1 \end{bmatrix}\begin{bmatrix} x(1) \\ x(2) \end{bmatrix}\right] \oplus \mathrm{Im}\left[\sqrt{\tfrac{2}{5}}\bigoplus_{k=0}^{4}\underline{V}_k\,\varepsilon_k^4\mathbf{x}_2\right] , \tag{2.9b}$$

where the $\oplus$ means direct sum, $x(1)$ and $x(2)$ are the amplitudes of the central atom, and $\underline{V}_k$ are as defined by formula (2.2.b).

III. DENSITY OF STATES

In this section, we apply the block-diagonal method presented in Sec. II to the study of the density of states for a Penrose lattice shown in Fig. 1. We consider atomic vibrations in the plane parallel to the Penrose lattice and deal with vibrations in the harmonic approximation. The equation of motion is written in terms of the dynamical matrix $\{D_{\alpha\beta}(l,l')\}$ as follows:

$$m_l\omega^2U^\alpha(l)=-\sum_{l',\beta}D_{\alpha\beta}(l,l')U^\beta(l') , \tag{3.1}$$

where m_l is the mass of the lth site in the αth atom, $U^\alpha(l)$ is the displacement of the atom at the lth site in the αth direction, and ω is the frequency of vibration.

In this paper, we investigate only the atomic vibrations in the plane parallel to the Penrose lattice and apply the Born model with central and angular forces considered.[16,20] First, we study the deformation of rhombi of the Penrose lattice, which is shown in Fig. 2. The potential energy due to the deformation can be resolved into two parts: V_c corresponds to the bond stretching and V_a due to the bond bending of rhombi; they are written, respectively, as follows:[16]

$$V_c=\tfrac{1}{2}\sum_{i,j}{}' k_{ij}[(\mathbf{u}_j-\mathbf{u}_i)\cdot\boldsymbol{\varepsilon}_{ij}]^2 , \tag{3.2a}$$

$$V_a=\tfrac{1}{2}\sum_{i,j,k}{}' \varepsilon_{ijk}(\boldsymbol{\varepsilon}_{ij}\times\mathbf{u}_j-\boldsymbol{\varepsilon}_{ij}\times\mathbf{u}_i-\boldsymbol{\varepsilon}_{ik}\times\mathbf{u}_k+\boldsymbol{\varepsilon}_{ik}\times\mathbf{u}_i)^2 , \tag{3.2b}$$

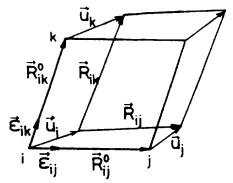

FIG. 2. Relative position vectors between lattice sites R_{ij}^0, displacement vectors of atoms u_i, and the relative position vectors between atoms R_{ij}, in a rhombus (Ref. 16).

where $\varepsilon_{ij}=\mathbf{R}_{ij}^0/|\mathbf{R}_{ij}^0|$, and k_{ij} and ε_{ijk} are the force constants of the central and the angular forces, respectively. The summation in Eq. (3.2a) is performed over all of the connected pairs; Eq. (3.2b) is carried out over all angles of the rhombi in the lattice.

The dynamical matrix elements $D_{ln}^{\alpha\beta}$ can be expressed as

$$D_{ln}^{\alpha\beta}=\frac{\partial^2 V_c}{\partial u_l^\alpha \partial u_n^\beta}+\frac{\partial^2 V_a}{\partial u_l^\alpha \partial u_n^\beta}=C_{ln}^{\alpha\beta}+A_{ln}^{\alpha\beta} . \tag{3.3}$$

Here we assumed that $k_{ij}=k$ and $\varepsilon_{ijk}=\varepsilon$, then the dynamical matrix elements $C_{ln}^{\alpha\beta}$ due to the bond stretching can be obtained as

$$C_{ln}^{\alpha\beta}=\delta_{ln}k\sum_{i\ (\neq l)}\varepsilon_{il}^\alpha\varepsilon_{il}^\beta-k\varepsilon_{nl}^\alpha\varepsilon_{nl}^\beta(1-\delta_{ln}) , \tag{3.4}$$

where the superscripts α and β denote the Cartesian coordinates. The dynamical matrix elements $A_{ln}^{\alpha\beta}$ due to the bond bending can be written as

$$A_{ln}^{\alpha\beta}=\tfrac{1}{2}\varepsilon\sum_{j,k}[(\varepsilon_{lk}^\alpha-\varepsilon_{lj}^\alpha)(\varepsilon_{lk}^\beta-\varepsilon_{lj}^\beta)-\delta^{\alpha\beta}(\varepsilon_{lk}^\gamma-\varepsilon_{lj}^\gamma)(\varepsilon_{lk}^\gamma-\varepsilon_{lk}^\gamma)]-\varepsilon\sum_{k,i}\left[\varepsilon_{il}^\alpha\varepsilon_{il}^\beta-\delta^{\alpha\beta}\sum_\gamma\varepsilon_{il}^\gamma\varepsilon_{il}^\gamma\right],\quad n=l ; \tag{3.5a}$$

$$A_{ln}^{\alpha\beta}=\varepsilon\sum_k\left[\varepsilon_{nl}^\alpha(\varepsilon_{lk}^\beta-\varepsilon_{ln}^\beta)-\delta^{\alpha\beta}\sum_\gamma\varepsilon_{ln}^\gamma(\varepsilon_{lk}^\gamma-\varepsilon_{ln}^\gamma)\right]-\varepsilon\sum_k\left[\varepsilon_{nl}^\beta(\varepsilon_{nk}^\alpha-\varepsilon_{nl}^\alpha)-\delta^{\alpha\beta}\sum_k\varepsilon_{nl}^\gamma(\varepsilon_{nk}^\gamma-\varepsilon_{nl}^\gamma)\right],\quad n=l\pm1 ; \tag{3.5b}$$

$$A_{ln}^{\alpha\beta}=\varepsilon\sum_i\left[\varepsilon_{in}^\beta\varepsilon_{il}^\beta-\delta^{\alpha\beta}\sum_\gamma\varepsilon_{in}^\gamma\varepsilon_{in}^\gamma\right],\quad n=l\pm2 . \tag{3.5c}$$

Equation (3.5b) is for the case that the lth and nth sites are nearest neighbors. Equation (3.5a) expresses the contribution of angular force to the diagonal elements, in which the summation over j and k are performed for the nearest neighbors of the lth site, and the sum over i for the second-nearest neighbors through the atom at the kth site. The sum is for the nearest neighbors of atoms at lth or nth site. Equation (3.5c) is for the second-nearest neighbors, in which the summation is performed over the nearest neighbors of both atoms at the lth and nth sites.

We have used the block-diagonal method presented in Sec. II and the equation of motion (3.1) to calculate numerically the eigenfrequencies and density of states, $D(\omega^2)$, for the Penrose lattice shown in Fig. 1 under the free boundary condition. The force constants k and ε are taken to be unity, respectively, and the masses of atoms are all the same and equal unity. The numerical results are shown in Fig. 3, in which it can be clearly seen that the spectral peaks appear at $\omega^2=2.5$, 9.3, 13.0, 17.1, 21.0, and 24.0, and a large gap appears near $\omega^2=24.0$. These results are in good agreement with those of Nishiguchi *et al.*, who have numerically studied the same system but did not use the block-diagonal method.[16]

IV. MEAN-SQUARE DISPLACEMENT AND MELTING

The study of melting of surfaces and interfaces is an active field of solid-state physics.[19–28] There exist several different criteria for the melting temperature. In this paper, we will use the mean-square-displacement (MSD) criterion of Lindemann to investigate the melting properties of two-dimensional Penrose lattices. MSD can be experimentally measured by using low-energy electron diffraction (LEED) or the Mössbauer effect, while it is also easier to tackle in a theoretical study. For crystals, when the amplitude of MSD reaches a critical fraction (10%) of the lattice constant, it is considered to start melting. By use of the Green's function, we can obtain an equation which relates the MSD, eigenvectors, and eigenvalues. Applying this equation to the two-dimensional Penrose system shown in Fig. 1, we first calculate the MSD for different kinds of atom, that is, we study the effects of coordination-number differences on the melting temperature.

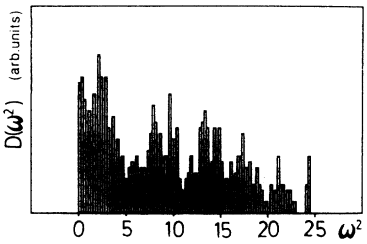

FIG. 3. Density of states of the lattice vibrations of the Penrose lattice studied (shown in Fig. 1). The force constants k and ε are taken to be unity. So are the atomic masses $M_i(I)=1$.

According to the equation of motion (3.1), we introduce a matrix

$$L_{\alpha\beta}(l,l')\equiv m_l\omega^2\delta_{\alpha\beta}\delta_{ll}+D_{\alpha\beta}(l,l') . \tag{4.1}$$

Let $\mathbf{U}=\{U^\alpha(l)\}$ denote the displacement vector; the equation of motion can be rewritten as

$$L\mathbf{U}=\mathbf{0} . \tag{4.2}$$

The phonon Green's function G satisfies the following equation:

$$LG=I , \tag{4.3}$$

where I is the unit tensor.

The relation between the atomic MSD and the phonon Green's function $G_{\alpha\beta}(l,l',-\Omega_n^2)$ simply is

$$\langle[U^\alpha(l)]^2\rangle=-(1/\beta)\sum_n G_{\alpha\alpha}(l,l,-\Omega_n^2) , \tag{4.4}$$

where $\Omega_n=2\pi nk_BT$ and $\beta=1/k_BT$, k_B is Boltzmann's constant, T is the temperature.[20]

In the high-temperature limit $T\gg T_D$, where T_D is an effective Debye temperature[22] for $n\neq0$, $G_{\alpha\alpha}(l,l,-\Omega_n^2)\simeq\Omega_n^{-2}$, so that the term with $n=0$ will make the main

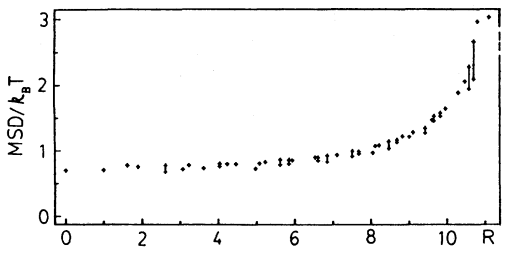

FIG. 4. Mean-square displacement (MSD) vs position parameter R for the Penrose lattice studied (shown in Fig. 1). The force constants k and ε are taken to be unity. So are the atomic masses $M_i(I)=1$.

contribution to the sum in Eq. (4.4), and the other terms can be neglected. Consequently, we have

$$\langle [U^{\alpha}(l)]^2 \rangle = -k_B T G_{\alpha\alpha}(l,l,0) , \tag{4.5}$$

If we have obtained the normalized eigenvectors $\{e_n^{\alpha}(l)\}$ and eigenfrequencies $\{\omega_n^2\}$ from Eq. (3.1), then the phonon Green's function can be expressed as

$$G_{\alpha\beta}(l,l',\omega^2)=\sum_n \frac{u_n^{\alpha *}(l)u_n^{\beta}(l')}{(\omega^2-\omega_n^2)} , \tag{4.6}$$

where $u_n^{\alpha}(l)=e_n^{\alpha}(l)/\sqrt{m_l}$. Then

$$G_{\alpha\alpha}(l,l',0)=-\sum_n [u_n^{\alpha *}(l)u_n^{\alpha}(l')]/\omega_n^2 . \tag{4.7}$$

From formulas (4.7) and (4.4), finally we have

$$\langle [U^{\alpha}(l)]^2 \rangle = k_B T \sum_n [u_n^{\alpha *}(l)u_n^{\alpha}(l)]/\omega_n^2 . \tag{4.8}$$

In what follows we apply the formula (4.8) to calculate the MSD of the Penrose lattice shown in Fig. 1.

We assume all atoms to have unit mass,

$$M_i(I)=1 , \tag{4.9}$$

where I is the coordination number of the ith atom. It means that for the eight kinds of vertex of these Penrose lattices, the located atoms have the same mass. Because the Penrose lattices being studied are circlelike and have rotational symmetry, in this case, it is natural to choose R, the distance from the ith vertex atom to the central atom, as its position parameter. The numerical results, which show the relationship between the MSD and the position parameter R, are plotted in Figs. 4 and 5. We can clearly see that the fluctuation of MSD is smaller in the bulk, but larger at the boundary. On the other hand, the MSD of boundary atoms are about three times as large as that of bulk atoms. It means that the boundary area will start melting before the bulk. This result is reasonable, and is the same as that of crystal systems.[20]

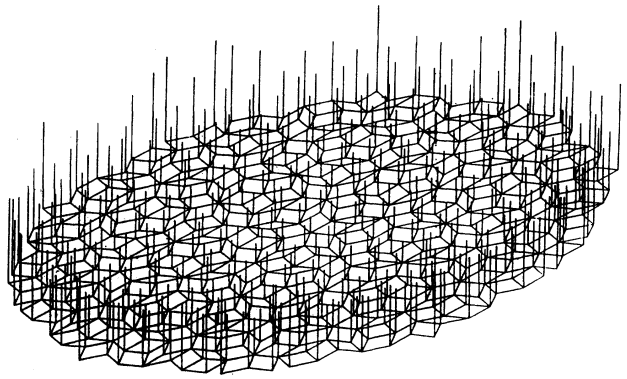

FIG. 5. Mean-square displacement of atoms located at the vertices of the Penrose lattice studied with atom number $N=471$. $k=\varepsilon=1$ and $M_i(I)=1$, as for Fig. 3.

We have also investigated the MSD difference among atoms with different coordination numbers but the same position parameter R. Table I shows that the atom with larger coordination number has smaller MSD. This result agrees with physical intuition: An atom with larger coordination number is more tightly bound by neighboring atoms. It also means that the crystals would have a higher melting temperature with stronger interactions among atoms.

Our conclusion that melting starts at the surface is based on the Lindemann criterion, and is therefore not final. A more comprehensive and definitive conclusion needs a more detailed and sophisticated theory, which is not at present available.

V. SUMMARY AND DISCUSSION

Based on the fivefold rotational symmetry of the two-dimensional Penrose lattices studied, a similarity transformation is introduced to make the dynamic matrix block-diagonal. This approach serves to reduce the computing time and computer memory required, and also allows us to determine analytically the degeneracy of the phonon modes. We have extended this approach to the general case of two-dimensional quasilattices with arbitrary N-fold rotational symmetry, and conclude that when N is even, $N-2$ out of the $N+2$ phonon modes are doubly degenerate and the remaining four phonon modes are nondegenerate. When N is odd, $N-1$ out of the $N+1$ phonon modes are doubly degenerate and the remaining two phonon modes are nondegenerate. In this way, we can easily use the block-diagonal approach presented in this paper to deal with the recently discovered two-dimensional quasicrystalline systems with eightfold,[8] tenfold,[9] and 12-fold[10] rotational symmetries.

We have obtained the relation among mean-square

TABLE I. Mean-square displacement (MSD) for different kinds of atom.

R	2.618		5.626		8.472		9.427		9.827	
Coordination Number	4	6	3	5	3	7	5	6	4	5
MSD (units of k_BT)	0.772	0.675	0.860	0.781	1.135	1.032	1.340	1.267	1.527	1.325

atomic displacement (MSD), eigenvectors, and eigenvalues of dynamical matrix. By using the MSD criterion of Lindemann, we have studied one case, in which the numerical results show that the boundary region does always start melting before the bulk and that atoms with larger coordination number will have smaller MSD, which means that they are more difficult to melt. These results are reasonable as the boundary atoms are less constricted than the bulk atoms. The melting properties of the quasicrystals are influenced by many other factors, such as the number of atomic species, atomic spacings, variable force constants, and alloy constituents. A more detailed study of the melting properties of quasicrystals, in both the experimental and theoretical aspects, is still necessary.

ACKNOWLEDGMENTS

This work was supported by the National Natural Science Foundation of China and in part by the International Program in Physical Science at Uppsala University, Sweden.

*Permanent address: Nanchang Army College, Nanchang 330103, P. R. China.

†Mailing address.

[1]D. Shechtman, I. Blech, D. Gratias, and J. Cahn, Phys. Rev. Lett. **53**, 1951 (1984).

[2]Z. Zhang, H. Q. Ye, and K. H. Kuo, Philos. Mag. **52**, 141 (1985).

[3]L. Bendersky, Phys. Rev. Lett. **55**, 1461 (1985).

[4]A. L. Mackay, Physica (Amsterdam) A **114**, 609 (1982).

[5]P. Kramer and R. Neri, Acta Crystallogr. Sec. A **40**, 580 (1984).

[6]V. Elser, Acta Crystallogr. Sec. A **42**, 36 (1986).

[7]D. Levine and P. J. Steinhardt, Phys. Rev. B **34**, 596 (1986).

[8]N. Wang, H. Chen, and K. H. Kuo, Phys. Rev. Lett. **59**, 1010 (1987).

[9]T. Ishimasa, H. U. Nissen, and Y. Fukano, Phys. Rev. Lett. **55**, 511 (1985).

[10]Q. V. Yang and W. D. Wei, Phys. Rev. Lett. **58**, 9 (1987).

[11]Penghui Ma and Youyan Liu, Phys. Rev. B **39**, 9904 (1989).

[12]Penghui Ma and Youyan Liu, Phys. Rev. B **39**, 10 658 (1989).

[13]T. Fujiwara, M. Aria, T. Tokihiro, and M. Kohmoto, Phys. Rev. B **37**, 2796 (1988).

[14]T. Odagaki and D. Nguyen, Phys. Rev. B **33**, 2184 (1986).

[15]M. Kohmoto and B. Sutherland, Phys. Rev. B **34**, 3849 (1986).

[16]N. Nishiguchi and T. Sakuma, Phys. Rev. B **38**, 7370 (1988).

[17]Youyan Liu and Penghui Ma, Phys. Rev. B **43**, 1378 (1991).

[18]J. E. S. Socolar and P. J. Steinhardt, Phys. Rev. B **34**, 617 (1986).

[19]J. W. M. Frenken and J. F. Van der Veen, Phys. Rev. Lett. **54**, 134 (1985).

[20]Changde Gong, Dingyu Xing, Arno Holz, and Jinzhong Pang, Phys. Rev. B **36**, 5517 (1987).

[21]Zou Nanzhi, Xing Dingyu, and Gong Changde, Commun. Theor. Phys. (Beijing, China) **4**, 425 (1987).

[22]F. A. Lindemann, Z. Phys. **14**, 609 (1910).

[23]*Handbook of Surface and Interfaces,* edited by A. A. Maraduduin, P. F. Wallis, and L. Dobrzynaski (Gorland STPM, New York, 1980), Vol. 3.

[24]S. Y. Tong, Prog. Surf. Sci. **7**, 1 (1977).

[25]L. Dobrzynski and J. Lajzerowicz, Phys. Rev. B **12**, 1358 (1975).

[26]R. F. Wallis, A. A. Maradudin, and L. Dobrzynski, Phys. Rev. B **15**, 5681 (1977).

[27]P. Mazur and A. A. Maradudin, Phys. Rev. B **24**, 2996 (1981).

[28]A. A. Maradudin and E. W. Montroll, *Theory of Lattice Dynamics in the Harmonics Approximation* (Academic, New York, 1971).